



Structural and magnetic properties of Nd₂NiGe₃



Sumanta Sarkar^a, Deepti Kalsi^a, Sudhindra Rayaprol^b, Sebastian C. Peter^{a,*}

^aNew Chemistry Unit, Jawaharlal Nehru Centre for Advanced Scientific Research, Jakkur, Bangalore 560064, India

^bUGC-DAE Consortium for Scientific Research, Mumbai Centre, R-5 Shed, BARC Campus, Mumbai 400085, India

ARTICLE INFO

Article history:

Received 26 November 2014

Received in revised form 1 January 2015

Accepted 21 January 2015

Available online 29 January 2015

Keywords:

Intermetallic

Crystal structure

Magnetism

X-ray diffraction

Neutron diffraction

ABSTRACT

Structural analysis of the room temperature diffraction data of Nd₂NiGe₃ shows that it exhibits AlB₂ type structure with space group *P6/mmm*. The crystal structure of Nd₂NiGe₃ consists of two dimensional Ni/Ge hexagonal units sandwiching the neodymium atoms between them. Temperature dependent magnetic susceptibility data follows Curie–Weiss law in the temperature range 20–300 K yielding an effective magnetic moment of 3.83 μ_B/Nd and paramagnetic Curie temperature −2.1 K indicating trivalent Nd and weak antiferromagnetic interactions, respectively. Low field magnetic susceptibility measurement show a weak antiferromagnetic like ordering around 3 K. Temperature dependent neutron diffraction measurements rules out long range antiferromagnetic ordering in this compound. The electrical resistivity measurement shows metallic nature of Nd₂NiGe₃, which exhibits sudden drop in resistivity below 3 K.

© 2015 Elsevier B.V. All rights reserved.

1. Introduction

Rare earth–transition metal based intermetallic compounds has been at focal point of researchers interested in the strongly correlated electron systems. Many of these systems show diverse crystal structures and wide range of physical properties, such as superconductivity, magnetic ordering (antiferromagnetism (AFM), ferromagnetism (FM)), spin-glass behavior, giant magnetoresistance (GMR), Kondo effect, heavy-fermions, thermoelectric and topological insulators [1–8]. The origins of these wide ranges of fascinating and anomalous physical properties are associated with the interplay of interactions between the localized 4f (or 5f) electrons of the rare earth atoms and the delocalized conduction electrons of the transition metal atoms. Among the RE–T–X (RE = rare earths, T = transition metals, X = p-block elements) intermetallics, compounds having general the formula RE₂TX₃ are extensively studied for their interesting structural and physical properties [9–23]. These compounds generally crystallize in the AlB₂ structure type and its ordered superstructures [24].

In our recent studies on this family of compounds, we came across variety of ordered compounds such as Eu₂AuSi₃, Eu₂AgGe₃, Eu₂AuGe₃, Yb₂AuSi₃ and Yb₂AuGe₃ [19–23] even though the disordered structures in these compositions were already reported in the literature [25–28]. Motivated by our findings, we have now undertaken a systematic study to determine the detailed crystallographic structure of some of the compounds in the AlB₂ structure

from whom ordered structures have been reported in the literature. In our recent investigations on Ce₂TGe₃ based compounds, we found ordered structure for Ce₂NiGe₃ [29] and disordered structure for Ce₂RhGe₃ (CeRh_{0.5}Ge_{1.5}) [30].

In the present study, we have chosen a neodymium (Nd) based compound, Nd₂NiGe₃. Some Nd based intermetallic systems have shown some interesting physical properties. Few examples of variety of Nd based intermetallics are: Nd₂Fe₁₄B is used as permanent magnet [31], magnetocaloric effect in NdMn₂Ge_{0.4}Si_{1.6} [32], low temperature cluster glass behavior in Nd₅Ge₃ [33], ferromagnetism and heavy fermion behavior in NdOs₄Sb₁₂ [34], metamagnetic behavior in Nd₃Pt₂₃Si₁₁ [35], magnetic-phase coexistence in Nd₇Rh₃ [36], etc.

A few Nd based compounds with other transition metals having the general formula RE₂TX₃ are reported in the literature. With the first row of transition metal, NdFe_{0.67}Ge_{1.33} [37], NdCo_{0.5}Ge_{1.5} [38], NdNi_xGe_(2-x) (x = 0.5 and 0.6) [39, 40] and NdCu_{0.71}Ge_{1.29} [41], with second row NdPd_{0.4}Ge_{1.6} [42], NdPd_{0.6}Ge_{1.4} [43], NdAg_{0.7}Ge_{1.3} [44], NdRh_{0.5}Ge_{1.5} [45] and NdRu_{1.2}Ge_{0.8} [46], and with third row only NdPt_{0.4}Ge_{1.6} [42] and NdIr_{0.5}Ge_{1.5} [42] were reported. All these compounds were studied only for the phase analysis by X-ray diffraction (XRD), except Nd₂PdGe₃, which was studied for magnetic properties [47].

The lack of detailed studies on these compounds motivated us to focus on the structure and properties in detail. We have selected the compound NdNi_{0.5}Ge_{1.5} which was first studied by Gladyshevskii and Bodak [48] considering the fact that both rare earth (Nd) and transition metal (Ni) atoms carry magnetic moment that can provide some interesting physical properties. Although earlier

* Corresponding author. Tel.: +91 80 22082998; fax: +91 80 22082627.

E-mail address: sebastiancp@jncasr.ac.in (S.C. Peter).

studies on the Nd–Ni–Ge phase by Salamakha et al. [40] suggested that no homogeneity range exists for this phase, our experience with similar compounds in this series had proved fruitful in generating compounds with varied stoichiometry by changing transition metal to p-block type metal. However, similar attempts in the case of Nd–Ni–Ge phase were not successful. The disordered compound $\text{NdNi}_x\text{Ge}_{(2-x)}$ [39, 40] are known to crystallize in the AlB_2 structure type with the substitution of the aluminum position by neodymium and the boron position shared by nickel and germanium atoms. Although the structure is disordered, we represent the compound as Nd_2NiGe_3 throughout the manuscript. The preliminary phase analysis of this compound was done by XRD. We have performed the magnetic and resistivity measurements on Nd_2NiGe_3 and discussed in detail. We have used neutron diffraction as complementary technique to support XRD and magnetization data.

2. Experimental details

2.1. Reagents

The following reagents were used as purchased without any further purification: rare earths (metal pieces, 99.99%, Alfa Aesar), Ni (wire, 99.99%, Alfa Aesar) and Ge (metal pieces, 99.999%, Alfa Aesar).

2.2. Synthesis

The elements were taken in the stoichiometric ratio and arc-melted in a water cooled copper hearth under argon atmosphere. The shiny globular ingots were formed as a result of arc, which was applied for 2–3 min. The globules were taken out, crushed and re-melted several times. Further homogenization of the sample was allowed by annealing it at 1173 K for 10 days. The product obtained was crushed and purity of the sample was checked by powder XRD.

2.3. X-ray diffraction (XRD)

Phase identity and purity of the Nd_2NiGe_3 samples were confirmed by powder X-ray diffraction carried out on a Bruker D8 Discover diffractometer using $\text{Cu K}\alpha$ radiation ($\lambda = 1.5406 \text{ \AA}$) and calibrated against corundum standard, over the angular range $20^\circ \leq 2\theta \leq 90^\circ$, with a step size of 0.02° at room temperature (300 K). Powder diffraction patterns were indexed using Le Bail method using the Fullprof program. Rietveld profile analysis in the Fullprof suite was used to refine the X-ray diffraction data. The background was estimated by the 6-coefficient polynomial function, and the peak shapes were described by a pseudo-Voigt function varying 10 profile parameters. A scale factor, a zero error factor and shape were refined. Cell constants were also refined during the process. Fig. 1 shows the XRD pattern for Nd_2NiGe_3 indexed on the basis of a hexagonal unit cell.

2.4. Elemental analysis

Semi-quantitative microanalyses were performed on the polycrystalline sample obtained from the arc melting using a scanning Leica 220i electron microscope (SEM) equipped with Bruker 129 eV energy dispersive X-ray analyzer (EDS). Data

were acquired with an accelerating voltage of 20 kV and in 90 s accumulation time. The average atomic composition obtained from the EDX analysis 33(3):23(3):44(3) for Nd:Ni:Ge is found to be very close to the expected composition of Nd_2NiGe_3 .

2.5. Neutron diffraction (ND)

ND patterns were recorded on well ground powder sample of Nd_2NiGe_3 . Sample was packed in a vanadium container and loaded in a closed cycle cryostat (CCR) for measuring ND patterns at temperatures between 2.8 and 300 K. The ND experiments were carried out on the focusing crystal diffractometer (FCD/PD-3) at Dhruva reactor, Trombay (India) using a wavelength of 1.48 \AA [49].

2.6. Magnetic measurements

Magnetic measurements on polycrystalline sample of Nd_2NiGe_3 were performed with a Quantum Design Magnetic Property Measurement System–Superconducting Quantum Interference Device (MPMS–SQUID) dc magnetometer. Temperature dependent magnetization data were collected in the field cooled (FC) as well as in zero field cooled (ZFC) modes in the temperature range 2–300 K in applied magnetic field of 1000 Oe. Temperature dependent ZFC–FC magnetization data were also recorded in low field ($H = 10 \text{ Oe}$) also. Magnetization as function of field was collected at 300 and 2 K for Nd_2NiGe_3 .

2.7. Resistivity measurements

The resistivity measurements were performed in zero field on Nd_2NiGe_3 with a conventional ac four probe set-up. Four very thin copper wires were glued to the pellet using a strongly conducting silver epoxy paste. The data were collected in the range 3–300 K using a commercial Quantum Design Physical Property Measurement System (QD–PPMS).

3. Results and discussion

3.1. Reaction chemistry

Motivated by our previous reports on the Ce compounds $\text{CeAu}_x\text{Ge}_{1-x}$ [50] and $\text{CeRh}_x\text{Ge}_{1-x}$ [30] in the formation of both hexagonal and tetragonal crystal systems by varying the ratio of transition metal and p-block elements, we have targeted the synthesis of the compounds with other rare earths. However, our attempts for the tetragonal system in Nd_2NiGe_3 were not successful. Nd_2NiGe_3 formed in the hexagonal system when the starting ratio was taken in 2:1:3. The compound also formed by varying the ratio of Ni to Ge, but, additional Ni or Ge were observed. All these phases could easily be identified in the XRD patterns. We also attempted to find the ordered structure similar to the one obtained for Ce_2NiGe_3 [29]. Since the compound was synthesized by arc melting, high quality single crystals were not obtained. In addition, our attempts to grow the single crystals by metal flux method (indium and tin as flux) were also unsuccessful. The compound is stable in air and no decomposition was observed even after several months. The elemental analysis of this compound with SEM/EDS gave the atomic composition, which is in good agreement with the ratio of the metals used for the synthesis.

3.2. Structural analysis

3.2.1. Crystal structure

Preliminary analysis of powder XRD confirms that the compound is a hexagonal system. Nd_2NiGe_3 was previously reported in the AlB_2 structure type with $P6/mmm$ space group [39]. In order to understand the detailed structure and properties, we have carried out ND studies as well. Structural analyses on XRD and ND data were carried out by Rietveld method using Fullprof suite program [51,52]. A preliminary refinement on the powder XRD data was carried out by adopting a reported structural model and indexed in the $P6/mmm$ space group and lattice parameters $a = b = 4.1445 \text{ \AA}$ and $c = 4.1823 \text{ \AA}$. Fig. 1 exhibits the Rietveld refined XRD patterns.

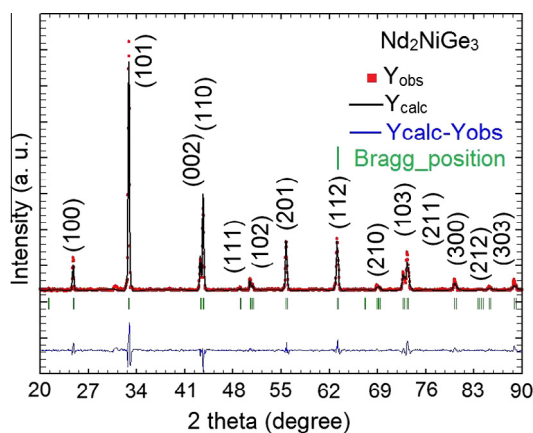


Fig. 1. Powder X-ray diffraction pattern for Nd_2NiGe_3 is shown here with miller indices for the Bragg peaks. The XRD pattern has been indexed on the basis of a hexagonal unit cell.

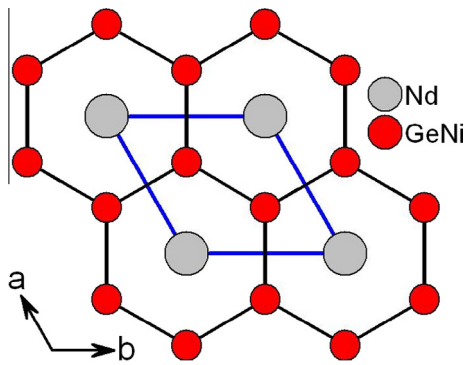


Fig. 2. Crystal structure of Nd_2NiGe_3 shown along the c -direction.

The crystal structure of Nd_2NiGe_3 along the c -direction is shown in Fig. 2. The compound crystallizes in the hexagonal AlB_2 structure type, space group $P6/mmm$. Nd atoms occupy the Al position while germanium and nickel atoms are statistically distributed in the boron position [53]. The crystal structure is composed of infinite arrays of planar hexagonal $[\text{NiGe}_3]$ units stacked along the $[001]$ direction and the Nd sites are sandwiched between these parallel hexagonal networks.

3.2.2. Neutron diffraction

Neutron diffraction measurements were carried out at various temperatures between 2.8 and 300 K. As can be seen from the magnetization measurements *vide infra*, there are no signatures of long-range magnetic ordering in this compound, similar to another compound of this series, Ce_2NiGe_3 [29]. ND data recorded at all temperatures were refined using the $P6/mmm$ structure as mentioned earlier and the details of the refinement are summarized in Table 1. The unit cell volume and cell parameters show decreasing trend from room temperature down to lowest temperature (see Fig. 3). There is however a very small anomaly observed in cell parameters around 15 K. At this moment the origin of this anomaly is not clear but can be speculated as a probable structural reorientation as expected for the compounds in the AlB_2 type and its ordered superstructures. At this context, this can be connected to the Bärnighausen formalism [54,55] proposed by Hoffmann and Pöttgen [24] for the group–subgroup relations in the AlB_2 family. As reported in the literature and our observations in few of our recent works, the ordering of the transition metal atoms and main

group elements at the boron positions in the planar hexagonal ring of the AlB_2 type may result in the loss of the basic hexagonal symmetry [18,24,56–58]. Depending on the extent of tilting and distortions of the hexagonal rings, these compounds may crystallize in the hexagonal, orthorhombic and monoclinic structures. This ordering and superstructure formation can be due to the size of the atoms, valence electron count and the nature of the bonding. The structural phase transition and associated with the magnetic properties in our recent works on the compounds Eu_2AuGe_3 , Eu_2AgGe_3 , Yb_2AuGe_3 [19,20,22].

In Fig. 4, Rietveld refinement profiles along with raw data are shown for ND patterns recorded at 2.8 and 300 K for direct comparison. As can be clearly seen from the figure, no additional Bragg peaks were observed in the case of 2.8 K profile when compared with the room temperature (300 K) profile. In addition, all the peaks in the pattern could be refined assuming the same structural model. Absence of any additional peak at 2.8 K thus rules out any long range antiferromagnetic order in this compound. Also, the intensities of the all Bragg peaks in the experimental data could be matched with calculated pattern using the crystallographic model itself thus ruling out any additional magnetic phase. Thus, considering the neutron diffraction and the magnetization data (discussed below) we expect that, similar to its Ce counterpart, the Nd compound is also a strong candidate for studying the magnetic properties using inelastic neutron scattering experiment.

3.3. Physical properties

3.3.1. Magnetic properties

The temperature dependent molar magnetic susceptibility and inverse susceptibility of Nd_2NiGe_3 is shown in Fig. 5. Magnetic moment was measured while warming in a field of 1 kOe after cooling the sample in presence and absence of applied magnetic field. Fitting the curve with Curie–Weiss law in the temperature range 20–300 K gives an effective magnetic moment (μ_{eff}) of $5.42 \mu_{\text{B}}/\text{f.u.}$, which turns out to be about $3.83 \mu_{\text{B}}/\text{Nd}$. The value of μ_{eff} per Nd atom is slightly higher than theoretical value ($3.62 \mu_{\text{B}}$) of the trivalent free Nd ion (considering $S = 3/2$, $L = 6$ and $J = 9/2$) [39]. The calculated paramagnetic Curie temperature (θ_p) is -2.1 K, which indicates antiferromagnetic interactions. With decreasing temperature, the magnetic susceptibility increases gradually but does not exhibit any sharp transition which could be considered as a magnetic ordering and hence this compound can be classified as a weak paramagnet or a Pauli paramagnet at

Table 1
Structural parameters obtained from the Rietveld refinement of neutron diffraction patterns of Nd_2NiGe_3 at temperatures between 2.8 K and 300 K. Space group: $P6/mmm$ (#191; general multiplicity = 24). Nd is at the atomic position $1a$ (000), and Ni/Ge are at $2d$ ($1/3, 2/3, 1/2$).

Parameters ↓	Temperature →										
	2.8 K	5 K	10 K	15 K	20 K	25 K	30 K	50 K	100 K	300 K	
a (Å)	4.1338 (5)	4.1338 (5)	4.1336 (5)	4.1340 (5)	4.1341 (5)	4.1341 (5)	4.1341 (5)	4.1342 (5)	4.1352 (4)	4.1425 (5)	
c (Å)	4.1712 (5)	4.1708 (5)	4.1710 (5)	4.1719 (5)	4.1718 (5)	4.1716 (5)	4.1716 (5)	4.1707 (5)	4.1725 (5)	4.1829 (5)	
c/a	1.0090	1.0089	1.0090	1.0091	1.0091	1.0090	1.0090	1.0088	1.0090	1.0097	
Volume (Å ³)	61.731 (3)	61.726 (3)	61.723 (3)	61.746 (3)	61.748 (3)	61.746 (3)	61.745 (3)	61.735 (3)	61.749 (3)	62.173 (3)	
B_{equ} (Å ²)											
Nd@ 1a	0.4622 (1)	0.4621 (1)	0.4621 (1)	0.4623 (1)	0.4623 (1)	0.4623 (1)	0.4623 (1)	0.4622 (1)	0.4625 (1)	0.4645 (1)	
Ni/Ge@ 2d	0.3990 (1)	0.4022 (1)	0.3722 (1)	0.4220 (1)	0.4393 (1)	0.4331 (1)	0.5050 (1)	0.4371 (1)	0.5045 (1)	0.8384 (1)	
<i>R</i> -parameters											
R_p	7.57	8.82	8.71	10.00	9.57	9.85	11.20	9.75	9.13	9.10	
R_{wp}	9.60	11.40	11.40	12.90	12.4	12.70	14.80	12.60	11.80	12.10	
R_{exp}	3.20	3.24	3.17	3.26	3.25	3.23	3.53	3.29	3.30	3.48	
χ^2	9.03	12.20	12.80	15.60	14.70	15.50	17.60	14.70	12.70	12.20	
Bragg- R	5.57	5.66	5.15	5.96	5.87	6.15	6.14	6.52	6.14	3.85	
R_f -factor	5.18	5.41	5.21	4.70	4.46	4.96	4.46	5.75	5.76	3.91	
GoF	3.00	3.50	3.60	4.40	4.20	4.20	4.50	3.80	3.80	3.40	

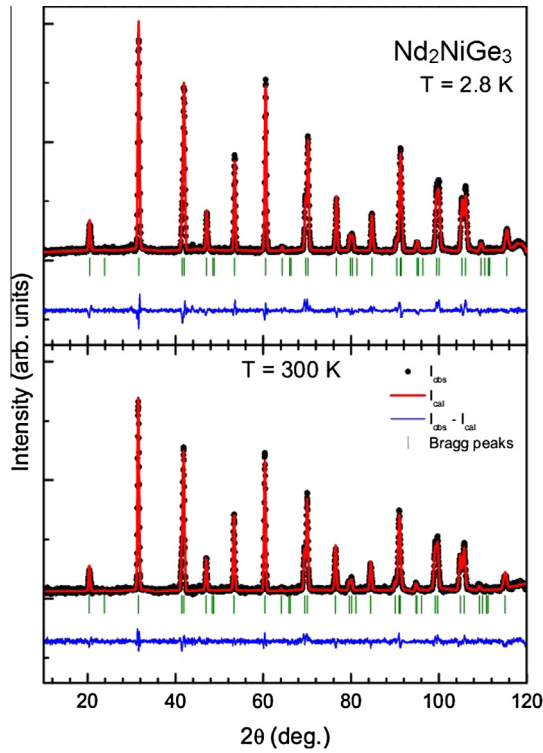


Fig. 3. Neutron diffraction patterns for the Nd_2NiGe_3 at 2.8 K and 300 K. The solid line through the experimental points is the Rietveld refinement pattern. The difference between the observed and the experimental pattern is shown in blue color and short vertical bars indicate the Bragg peak positions. (For interpretation of the references to colour in this figure legend, the reader is referred to the web version of this article.)

this field [39]. Low field magnetic susceptibility measurements were also carried out in ZFC–FC modes. A sharp upturn can be observed at very low magnetic field ($H = 10$ Oe) in the ZFC curve, as shown in the inset of Fig. 5. In FC curve, below 3 K, the curve does not decrease with further lowering of temperature, instead it rather saturates as if independent of temperature below 3 K. The difference in ZFC–FC curves indicates the strong magnetic anisotropy in this system, indicating spin-glass like state below 3 K in this system.

The field dependence of magnetic moment at 300 and 2 K is shown in Fig. 6. The high temperature curve increases linearly as expected for a paramagnet in a Curie–Weiss regime. At low temperature (2 K), the moment, however, increases sharply up to 30 kOe followed by a curvature. The moment however does not saturate up to the highest applied field and is calculated to be $2.2 \mu_B$ which is around 61% of the expected value indicating the presence of crystalline field effect in this compound resulting in the reduction of the expected saturation magnetization value. The S-shape of the magnetization loop is also an indication that the system is a spin-glass at this temperature.

3.3.2. Resistivity

The temperature dependent electrical resistivity of the Nd_2NiGe_3 sample in the temperature range 3–300 K is shown in Fig. 7. In the low temperature range, there is a sudden drop in resistivity near 3 K and it sharply decreases with further decrease in temperature. This could arise due to onset of ferromagnetic ordering as also observed in another AlB_2 type compound, Eu_2CuSi_3 [59,60]. At temperatures below 10 K, the $\rho(T)$ data can be fitted to the power law function, $\rho = \rho_0 + AT^n$, where ρ_0 is the residual resistivity expressed

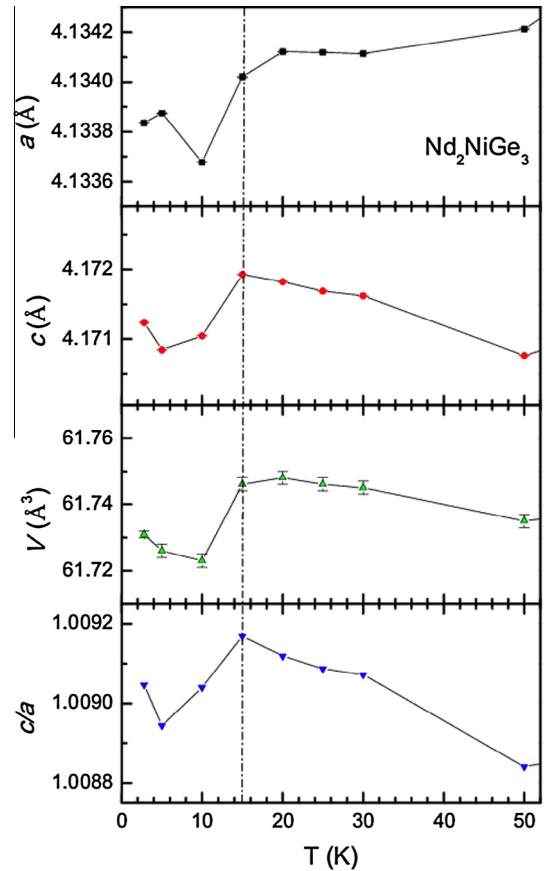


Fig. 4. Variation of cell parameters as a function of temperature is plotted in different forms. The vertical dashed line is drawn to show the highlight the temperature at which anomaly occurs in the cell parameters.

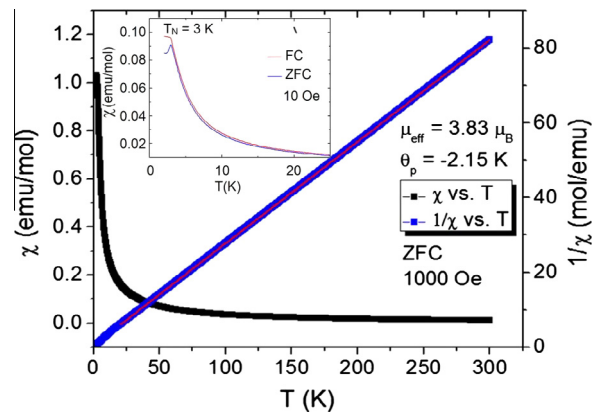


Fig. 5. Temperature dependence of magnetic susceptibility and inverse magnetic susceptibility measured in 1 kOe applied dc magnetic field. The inset shows temperature dependence of magnetic susceptibility in zero field cooled (ZFC) and field cooled (FC) modes at 10 Oe.

in units of $\mu\Omega$ cm and A and n are the fitting parameters [61]. The residual resistivity (ρ_0) was $6.4 \mu\Omega$ cm and power factor was 0.48. The low value of n hints that the conduction electrons are not strongly correlated to the localized $4f$ orbitals and the system shows non-Fermi liquid behavior (NFL) [62] i.e. it does not behave like a Fermi liquid in its ground state, in that case the power value would have been closer to two [63]. The residual resistivity ratio (RRR),

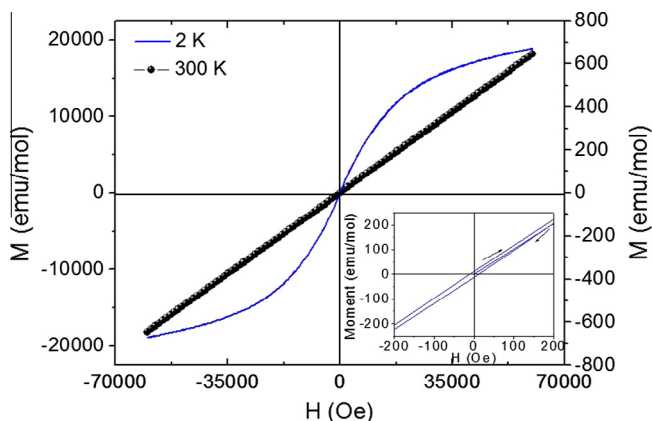


Fig. 6. Field dependence of magnetic moment at 2 and 300 K. The inset shows low field ranges of the magnetization curve.

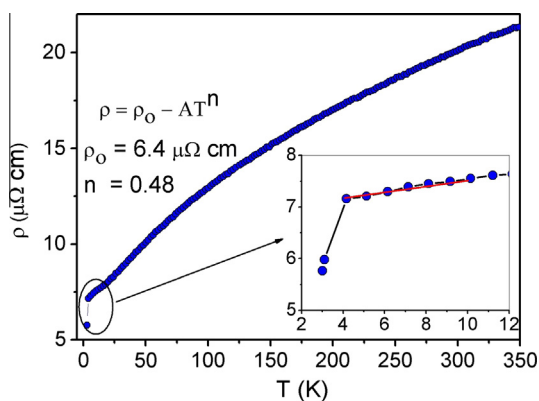


Fig. 7. Resistivity (ρ) measured as a function of temperature in zero field. The inset figure shows the low temperature behavior and red line shows the fitting range. (For interpretation of the references to colour in this figure legend, the reader is referred to the web version of this article.)

ρ_{300}/ρ_0 for this compound is 3.2, considerably higher than 1, indicates that the sample purity is quite high and defect free [21].

4. Concluding remarks

The compound Nd_2NiGe_3 was obtained in pure form by arc melting. The crystal structure of this compound was studied by X-ray and neutron diffraction studies. Our preliminary magnetic and resistivity measurements suggest short-range magnetic ordering and probable non-Fermi liquid behavior suggest that spin-orbit interaction exists in this compound, which needs to be further studies different probes such as neutron inelastic scattering experiments. Though the expected ordered compound was not formed, our work is just a mere start of searching interesting physical properties lying on several Nd based compounds reported only by XRD.

Acknowledgments

We thank JNCASR, UGC-DAE CSR (Project No. CRS-M-166) and Sheikh Saqr Laboratory for the financial support. S.S. thanks CSIR for research fellowship D.K. thanks the UGC-DAE CSR, Mumbai center for Project fellowship, and S.C.P. thanks to DST for Ramanujan fellowship (Grant SR/S2/RJN-24/2010). We are grateful to Prof. C.N.R. Rao for his constant support and encouragement.

References

- [1] R.J. Cava, H.W. Zandbergen, B. Batlogg, H. Eisaki, H. Takagi, J.J. Krajewski, W.F. Peck, E.M. Gyorgy, S. Uchida, *Nature* 372 (1994) 245–247.
- [2] Y.F. Yang, Z. Fisk, H.O. Lee, J.D. Thompson, D. Pines, *Nature* 454 (2008) 611–613.
- [3] S. Chadov, X.L. Qi, J. Kubler, G.H. Fecher, C. Felser, S.C. Zhang, *Nat. Mater.* 9 (2010) 541–545.
- [4] K. Kamishima, T. Goto, H. Nakagawa, N. Miura, M. Ohashi, N. Mori, T. Sasaki, T. Kanomata, *Phys. Rev. B* 63 (2001).
- [5] M. Jourdan, M. Huth, H. Adrian, *Nature* 398 (1999) 47–49.
- [6] O. Stockert, J. Arndt, E. Faulhaber, C. Geibel, H.S. Jeevan, S. Kirchner, M. Loewenhaupt, K. Schmalzl, W. Schmidt, Q. Si, F. Steglich, *Nat. Phys.* 7 (2011) 119–124.
- [7] S.R. Brown, S.M. Kauzlarich, F. Gascoin, G.J. Snyder, *Chem. Mater.* 18 (2006) 1873–1877.
- [8] E.M. Benbow, N.S. Dalal, S.E. Latturmer, *J. Am. Chem. Soc.* 131 (2009) 3349–3354.
- [9] K. Mukherjee, T. Basu, K.K. Iyer, E.V. Sampathkumaran, *AIP Conf. Proc.* 1447 (2012) 1097–1098.
- [10] S. Patil, V.R.R. Medicherla, R.S. Singh, S.K. Pandey, E.V. Sampathkumaran, K. Maiti, *Phys. Rev. B* 82 (2010).
- [11] E.V. Sampathkumaran, S. Majumdar, W. Schneider, S.L. Molodtsov, C. Laubschat, *Physica B* 312 (2002) 152–154.
- [12] S. Majumdar, E.V. Sampathkumaran, *Phys. Rev. B* 63 (2001).
- [13] S. Majumdar, E.V. Sampathkumaran, *Solid State Commun.* 117 (2001) 645–648.
- [14] E.V. Sampathkumaran, I. Das, R. Rawat, S. Majumdar, *Appl. Phys. Lett.* 77 (2000) 418–420.
- [15] S.R. Saha, H. Sugawara, T.D. Matsuda, Y. Aoki, H. Sato, E.V. Sampathkumaran, *Phys. Rev. B* 62 (2000) 425–429.
- [16] S. Majumdar, E.V. Sampathkumaran, *Phys. Rev. B* 61 (2000) 43–45.
- [17] S. Majumdar, M.M. Kumar, E.V. Sampathkumaran, *J. Alloys Comp.* 288 (1999) 61–64.
- [18] R. Mallik, E.V. Sampathkumaran, P.L. Paulose, *Solid State Commun.* 106 (1998) 169–172.
- [19] C.P. Sebastian, C.D. Malliakas, M. Chondroudi, I. Schellenberg, S. Rayaprol, R.D. Hoffmann, R. Pöttgen, M.G. Kanatzidis, *Inorg. Chem.* 49 (2010) 9574–9580.
- [20] S.C. Peter, S. Sarkar, M.G. Kanatzidis, *Inorg. Chem.* 51 (2012) 10793–10799.
- [21] S. Sarkar, M.J. Gutmann, S.C. Peter, *Cryst. Growth Des.* 13 (2013) 4285–4294.
- [22] S. Sarkar, S.C. Peter, *Inorg. Chem.* 52 (2013) 9741–9748.
- [23] S. Sarkar, M.J. Gutmann, S.C. Peter, *CrystEngComm* 15 (2013) 8006–8013.
- [24] R.D. Hoffmann, R. Pöttgen, *Z. Kristallogr.* 216 (2001) 127–145.
- [25] I. Mayer, I. Felner, *J. Solid State Chem.* 8 (1973) 355–356.
- [26] F. Merlo, M. Pani, F. Canepa, M.L. Fornasini, *J. Alloys Comp.* 264 (1998) 82–88.
- [27] M. Pani, F. Merlo, M.L. Fornasini, *Z. Kristallogr.* 214 (1999) 108–110.
- [28] R. Pöttgen, B. Gibson, R.K. Kremer, *Z. Kristallogr.* 212 (1997), 58.
- [29] D. Kalsi, S. Rayaprol, V. Siruguri, S.C. Peter, *J. Solid State Chem.* 217 (2014) 113–119.
- [30] D. Kalsi, U. Subbarao, S. Rayaprol, S.C. Peter, *J. Solid State Chem.* 212 (2014) 73–80.
- [31] J.F. Herbst, J.J. Croat, F.E. Pinkerton, W.B. Yelon, *Phys. Rev. B* 29 (1984) 4176–4178.
- [32] J.L. Wang, S.J. Campbell, J.M. Cadogan, A.J. Studer, R. Zeng, S.X. Dou, *Appl. Phys. Lett.* 98 (2011) 232509.
- [33] B. Maji, K.G. Suresh, A.K. Nigam, *J. Phys.: Condens. Matter.* 23 (2011) 506002.
- [34] P.-C. Ho, W.M. Yuhasz, N.P. Butch, N.A. Frederick, T.A. Sayles, J.R. Jeffries, M.B. Maple, J.B. Betts, A.H. Lacerda, P. Rogl, G. Giester, *Phys. Rev. B* 72 (2005) 094410.
- [35] C. Opagiste, M.J. Jackson, R.M. Galéra, E. Lhotel, C. Paulsen, B. Ouladdiaf, *J. Magn. Magn. Mat.* 340 (2013) 46–49.
- [36] S. Rayaprol, V. Siruguri, A. Hoser, C. Ritter, E.V. Sampathkumaran, *Phys. Rev. B* 90 (2014) 134417.
- [37] I. Mayer, I. Felner, *Solid State Commun.* 13 (1973) 457–461.
- [38] P.S. Salamakha, *J. Alloys Comp.* 255 (1997) 209–220.
- [39] J.W. Chen, S.Y. Guan, C.H. Wang, *J. Phys.: Conf. Ser.* 266 (2011) 012006.
- [40] P.S. Salamakha, M.B. Konyk, O.L. Sologub, O.I. Bodak, *J. Alloys Comp.* 236 (1996) 206–211.
- [41] P.S. Salamakha, *Visn. L'viv. Derzh. Univ. (Ser. Khim.)* (1986) 27.
- [42] P.S. Salamakha, O.I. Bodak, V.K. Pecharskii, V.K. Bel'skii, *Russ. Metall.* 1 (1989) 210–212.
- [43] G. Bocelli, O.L. Sologub, P.S. Salamakha, *J. Alloys Comp.* 360 (2003) L3–L6.
- [44] O.V. Zaplatynsky, P.S. Salamakha, O.L. Sologub, O.S. Procyk, O.I. Bodak, *Pol. J. Chem.* 70 (1996) 267–269.
- [45] P.S. Salamakha, O.I. Bodak, V.K. Percharkii, V.K. Belskii, *Russ. Metall.* (1989) 210–212.
- [46] C. Rizzoli, O.L. Sologub, P. Salamakha, *J. Alloys Comp.* 350 (2003) 160–163.
- [47] S. Majumdar, E.V. Sampathkumaran, *Phys. Rev. B* 63 (2001) 172407.
- [48] E.I. Gladyshevskii, O.I. Bodak, *Dopov. Akad. Nauk Ukr. RSR* 14 (1965).
- [49] V. Siruguri, P.D. Babu, M. Gupta, A.V. Pimpale, P.S. Goyal, *Pramana – J. Phys.* 71 (2008) 1197–1202.
- [50] C.P. Sebastian, M.G. Kanatzidis, *J. Solid State Chem.* 183 (2010) 878–882.
- [51] H.M. Rietveld, *J. Appl. Crystallogr.* 2 (1969) 65.
- [52] J. Rodriguez-Carvajal, *Physica B* 192 (1993) 55.

- [53] B. Chevalier, R. Pottgen, B. Darriet, P. Gravereau, J. Etourneau, J. Alloys Comp. 233 (1996) 150–160.
- [54] H. Bärnighausen, Commun. Math. Chem. 9 (1980) 139–175.
- [55] H. Bärnighausen, U. Müller, Universität Karlsruhe and Universität-Gh Kassel, Germany, 1996.
- [56] R. Mallik, E.V. Sampathkumaran, M. Strecker, G. Wortmann, P.L. Paulose, Y. Ueda, J. Magn. Magn. Mater. 185 (1998) L135–L143.
- [57] E.V. Sampathkumaran, H. Bitterlich, K.K. Iyer, W. Loser, G. Behr, Phys. Rev. B 66 (2002) 052409.
- [58] K.K. Iyer, P.L. Paulose, E.V. Sampathkumaran, M. Frontzek, A. Kreyssig, M. Doerr, M. Loewenhaupt, I. Mazilu, G. Behr, W. Loser, Physica B 355 (2005) 158–163.
- [59] C.D. Cao, R. Klingeler, H. Vinzelberg, N. Leps, W. Löser, G. Behr, F. Muranyi, V. Kataev, B. Büchner, Phys. Rev. B 82 (2010) 134446.
- [60] S. Majumdar, R. Mallik, E.V. Sampathkumaran, K. Rupprecht, G. Wortmann, Phys. Rev. B 60 (1999) 6770–6774.
- [61] S. Kambe, H. Suderow, T. Fukuhara, J. Flouquet, T. Takimoto, J. Low Temp. Phys. 117 (1999) 101–112.
- [62] G. Stewart, Rev. Mod. Phys. 73 (2001) 797–855.
- [63] P. Coleman, Introduction to Many Body Physics, In Rutgers University Press, USA, 2004.